Inorganic Chemistry

ARTICLE

pubs.acs.org/IC

High-Pressure Synthesis and Superconductivity of a New Binary Lanthanum Germanide $LaGe_3$ with Triangular Ge_3 Cluster Units

Hiroshi Fukuoka,*[,†] Koichiro Suekuni,[‡] Takahiro Onimaru,[‡] and Kei Inumaru[†]

[†]Department of Applied Chemistry, Faculty of Engineering, Hiroshima University, Higashi-Hiroshima 739-8527, Japan

[‡]Department of Quantum Matter, ADMS, Hiroshima University, Higashi-Hiroshima 739-8530, Japan

ABSTRACT: We prepared a new binary lanthanum germanide, $LaGe_3$, under high-pressure and high-temperature conditions (3−12 GPa, 500−1200 °C). It crystallizes in the $BaPb_3$ structure (the space group $R\bar{3}m$) with lattice constants of $a = 6.376(1)$ Å, $c = 22.272(3)$ Å, and $V = 784.1(2)$ Å^3. We refined the structure using Rietveld analysis from X-ray powder data. The structure is composed of two types of close-packed atom layers. In one layer, every La atom is surrounded solely by Ge atoms with the same distance of 3.188 Å. The other layer contains Ge_3 regular, triangular cluster units with a Ge−Ge distance of 2.634 Å. The electron localization function and crystal orbital Hamilton population calculations suggest that the triangular cluster is composed of three Ge−Ge covalent bonds and that each Ge atom has a lone pair. The temperature dependence of the magnetic susceptibility and electrical conductivity measurements revealed that $LaGe_3$ is metallic and shows superconductivity at 7.4 K. This critical temperature is highest for the La−Ge system.

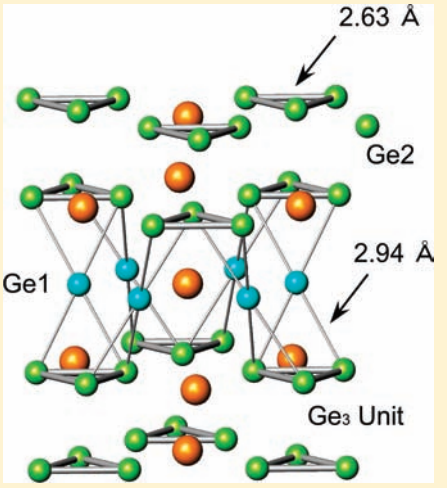

INTRODUCTION

Reactions of electropositive metals (alkaline, alkaline earth, and rare earth metals) and some p-block elements often yield compounds containing subunits of the p-block atoms. The p-block atoms are negatively charged due to the electrons donated by the metals. Some of the electrons are used by the p-block atoms to form covalent bonds, and the resultant subunits demonstrate abundant structural variations, including one-dimensional (1D) cluster anions, two-dimensional (2D) layer sheets, and three-dimensional (3D) networks.[1−4] The metal atoms become cations and reside in the spaces of the subunits. Zintl phases are typical examples of such compounds,[1] and the cluster anions are called Zintl anions.[2] These types of compounds are formed by both covalent and ionic interactions.

Host atoms (relatively electronegative atoms) that construct subunits in Zintl phases often fulfill the eight-electron rule and have closed-shell structures. These compounds, therefore, possess semiconducting properties. On the other hand, several metallic compounds with similar combinations of elements have been reported.[5,6] They contain similar or in some cases identical subunits, but the host atoms do not fulfill the 8-electron rule and, therefore, possess metallic or semimetallic properties.

These metallic compounds are not categorized into typical or classical Zintl phases. We are interested in such compounds because metallic Zintl phases sometimes demonstrate interesting physical properties such as superconductivity. We investigated reactions of group 14 and 15 elements and alkali, alkaline earth, and lanthanide metals. High-pressure synthesis is a powerful method to obtain new compounds, especially silicides and germanides, having interesting structures and physical properties.

Typical examples of such metallic compounds are silicon clathrates. $Ba_{8-x}Si_{46}$, prepared by reactions at 3 GPa and 800 °C,[7] has the type-I clathrate structure[8−10] composed of pentagonal dodecahedral Si_{20} cages with Ba atoms at the center. This 3D host structure is composed of a covalent network of sp^3 Si atoms only.

$Ba_{8-x}Si_{46}$ is isotypic with K_8Si_{44}. However, in the potassium silicide, there are 2 Si vacancies per 46 Si sites.[11] According to the Zintl−Klemm concept,[1,12,13] all Si atoms in K_8Si_{44} have closed-shell structures, and in fact, the compound is a semiconductor. A lot of type-I silicon and germanium clathrate compounds follow the Zintl−Klemm rule and show semiconducting or poor metallic properties (Ba_8Ge_{46-x}, $Ba_8Al_{16}Si_{30}$, etc).[14−20]

Binary silicon clathrate, $Ba_{8-x}Si_{46}$, however, has no vacancy in the host network. The electrons donated from Ba become conduction electrons. In fact, $Ba_{8-x}Si_{46}$ is metallic and shows a superconducting transition at 5−9 K depending on the amount of Ba vacancy x.[21] This compound has attracted much attention because it is the first superconductor with a network composed of four-bonded sp^3 silicon atoms only.[22−25] Another type of silicon clathrate, $Ba_{24}Si_{100}$, is prepared by high-pressure synthesis (1.5 GPa, 800 °C) and becomes a superconductor at 1.4 K.[26,27]

Received: October 13, 2010
Published: March 29, 2011

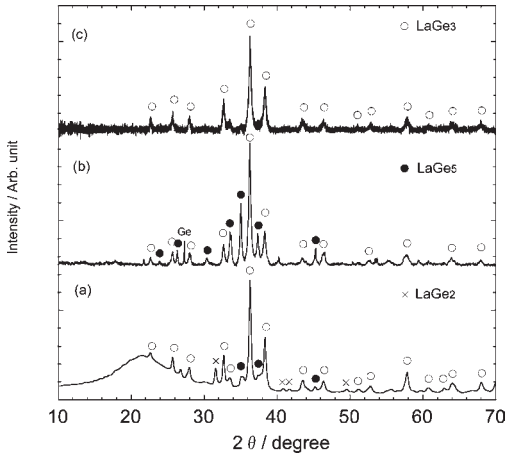

Figure 1. X-ray powder diffraction patterns of La−Ge samples: (a) 5 GPa, 500 °C; (b) 12 GPa, 1100 °C; (c) 10 GPa, 850 °C. Cross marks show diffractions from $LaGe_2$. Filled and open circles show XRD patterns of $LaGe_5$ and $LaGe_3$, respectively.

In our studies of germanides, we obtained many metallic germanides of alkaline and rare earth elements. $Ba_{24}Ge_{100}$ and $LaGe_5$ become superconductors at 0.27 and 6.8 K, respectively.[27,28] $Ba_{24}Ge_{100}$, isotypic with $Ba_{24}Si_{100}$, was prepared by simple arc melting.[29−31] Recently, a new clathrate compound $BaGe_5$ was reported by another group. This is not a metallic but a semiconducting Zintl phase.[32] We prepared a lanthanum pentagermanide, $LaGe_5$, under high-pressure (5 GPa) conditions.[28] An isotypic series of $LnGe_5$ (Ln = Ce, Pr, Nd, and Sm) was also prepared under similar conditions.[33] They contain six-membered Ge rings in a boat conformation that share their edges to form puckered layers. The layers are connected by 8-fold Ge atoms to form tunnels where Ln atoms are situated. The coordination number of eight is extremely large for Ge atoms, which is possibly an effect of the high pressure. All $LnGe_5$ compounds are metallic, but only $LaGe_5$ shows superconductivity.

We noticed a new phase on investigating the $LaGe_5$ synthesis. We attempted to characterize this new compound. In this study, we performed a detailed investigation of the reactions between La and Ge under high-pressure conditions and found a new binary lanthanum germanide, $LaGe_3$, having a Ge_3 triangular cluster unit. This is the first triangular Zintl anion of Ge to our knowledge. We examined the structure and electrical and thermal properties of $LaGe_3$ and discussed the electronic structure of the unit using first-principle calculations.

EXPERIMENTAL SECTION

$LaGe_3$ was prepared using a two-step reaction as follows: a mixture of La (Furu-uchi Chemical 99.9%) and Ge (Mitsuwa Pure Chemical 99.999%) in a 1:3 atomic ratio was reacted in an Ar-filled arc furnace to obtain a mixture of $LaGe_2$ and Ge. The mixture was well ground in an agate mortar and then placed in an h-BN cell. It was reacted using a Kawai-type high-pressure system.[34] We performed reactions varying both temperature (500−1600 °C) and pressure (3−13 GPa). The products were characterized using X-ray powder diffraction (XRD) measurements with a Bruker AXS D8 Advance diffractometer with Ni-filtered Cu Kα radiation. The data for structural analysis were collected using the step-scan mode (0.00741°) from 24° to 100°. A nonreflecting Si plate was used as a sample holder in order to reduce the background. The structure refinement was performed using RIETAN2000, a multipurpose pattern-fitting system.[35]

Table 1. Crystallographic Data of $LaGe_3$ and *R* Indices of Rietveld Analysis[a]

formula	$LaGe_3$
space group	$R\bar{3}m$(166)
lattice parameter a/Å	6.376(1)
lattice parameter c/Å	22.272(3)
unit cell volume V/Å^3	784.1(2)
2θ range/deg	24−100
R_{wp}/%	4.47
R_P/%	3.54
R_E/%	3.09
R_I/%	0.65
R_F/%	0.32
goodness of fit S	1.45

[a] $R_{wp} = [\Sigma_i w_i\{y_i - I_i\}^2/\Sigma_i w_i y_i^2]^{1/2}$. $R_p = \Sigma_i |y_i - I_i|/\Sigma_i y_i$. $R_e = [(N - P)/\Sigma_i w_i y_i^2]^{1/2}$. $R_I = \Sigma_k |I_k(\text{'o'}) - I_k(\text{c})|/\Sigma_k I_k(\text{'o'})$. $R_F = \Sigma_k | [I_k(\text{'o'})]^{1/2} - [I_k(\text{c})]^{1/2}|/\Sigma_k [I_k(\text{'o'})]^{1/2}$. $S = R_{wp}/R_e$. y_i: observed intensity. I_i: calculated intensity. w_i: weight. N: number of data points. P: number of parameters. $I_k(\text{'o'})$: estimated observed intensity of the kth reflection. $I_k(\text{c})$: calculated intensity of the kth reflection.

Table 2. Atomic Parameters of $LaGe_3$ Refined by the Rietveld Method

atom	site	x	y	z	B_{eq}
La1	3a	0	0	0	0.2(3)
La2	6c	0	0	0.2172(2)	1.2(3)
Ge1	9e	1/2	0	0	0.3(3)
Ge2	18 h	0.1956(3)	0.8044	0.1078(2)	0.6(2)

Chemical compositions of the products were examined using an electron probe microanalyzer (EPMA) (JEOL JCMA-733). Magnetic susceptibility measurements were performed with a SQUID magnetometer (Quantum Design MPMS-5) in a 20-Oe field.

Electrical resistivity was measured on a rectangular-shaped specimen with dimensions of 2.40 × 1.00 × 0.50 mm prepared by polishing the obtained bulk product with sandpaper. We measured the resistivity of the specimen with the four-probe method using DC from room temperature to 2 K. The specific heat was measured from 4 to 200 K on a Quantum Design physical property measurement system using its standard thermal-relaxation method.

The band structure calculation was performed using the WIEN2k package with a general potential LAPW code.[36] Some parameters used were as follows: RMT, 2.5 for La and 2.47 for Ge; G_{max}, 12; RMT × k_{max}, 7; number of k points, 10 000. Electron localization functional (ELF) and chemical bond analysis using COHP techniques were calculated and analyzed using a tight-binding linear muffin-tin orbital-atomic sphere approximation with TB-LMTO-ASA software.[37]

RESULTS AND DISCUSSION

The XRD pattern of the product obtained by reaction at 5 GPa and 500 °C for 1 h is shown in Figure 1a. Although some small peaks were caused by $LaGe_5$ and $LaGe_2$, the main peaks could not be identified as any known phases. The peaks were successfully indexed using a hexagonal cell with a = 6.381(1) Å and c = 22.290(3) Å. The increase of pressure and temperature to 12 GPa and 1100 °C improved the crystallinity of the unknown phase, but the content of $LaGe_5$ also increased as shown in Figure 1b. We obtained the best sample of the unknown phase by a reaction at 10 GPa and 850 °C for 1 h (see Figure 1c). We

dx.doi.org/10.1021/ic102077k |*Inorg. Chem.* 2011, 50, 3901–3906

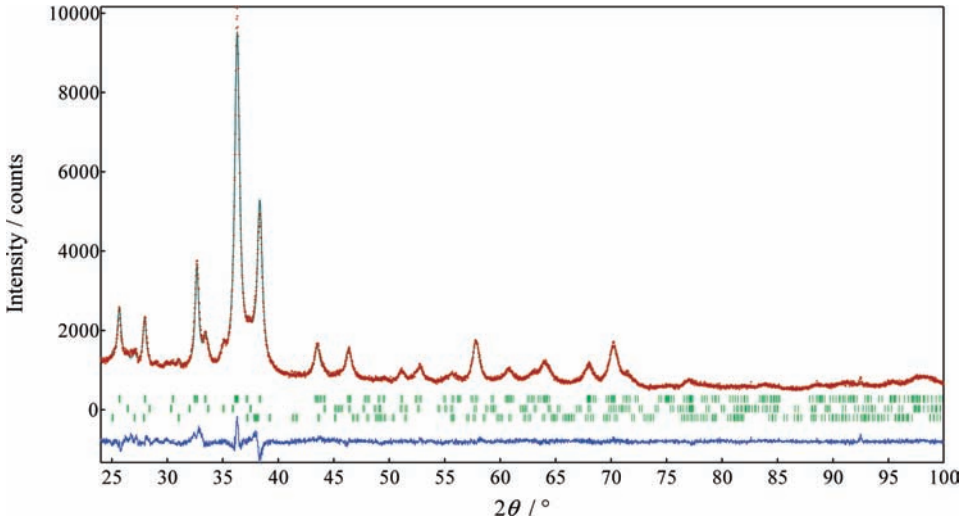

Figure 2. Fitting result of Rietveld analysis of $LaGe_3$. The observed data are shown as small red crosses and the calculated fits and difference curves as solid lines. Tick marks indicate calculated peak positions. They are for $LaGe_3$, $LaGe_5$, and $LaGe_2$ sequentially from the top.

performed chemical analysis of the unknown phase using EPMA and obtained a composition of La:Ge = 1:2.91(3), suggesting that a new lanthanum germanide, $LaGe_3$, had been prepared by the high-pressure and high-temperature reactions. The compound is very stable against air and moisture under ambient pressure.

Several structures having the AB_3 composition have been reported including the Cu_3Au, $BaSn_3$, $BaPb_3$, and $SrSn_3$ structures.[38−40] From the detailed study of the XRD pattern, the unknown phase seemed to be isotypic with $BaPb_3$, which has a trigonal unit cell with the space group of $R\bar{3}m$.[39] In order to confirm the structure, we performed Rietveld analysis on the sample shown in Figure 1c using the atomic parameters of $BaPb_3$ as the initial values. As both $LaGe_5$ and $LaGe_2$ having very poor crystallinities were detected as minor products in the sample, we performed the refinement including these phases. Overall isotropic displacement parameters were adopted individually for the minor products $LaGe_5$ and $LaGe_2$. The final refinement was well converged and gave good R indices. Therefore, we concluded that the unknown phase was $LaGe_3$ with the $BaPb_3$-type structure. The crystallographic data and results of the pattern fitting of the Rietveld analysis are presented in Tables 1 and 2 and Figure 2.

The crystal structure of $LaGe_3$ projected along the c axis is presented in Figure 3a. If the distinction of La and Ge atoms is disregarded, this structure can be seen as a closest packing structure. Figure 3b depicts how each layer is stacked. The unit cell along the c axis contains nine layers. There are two kinds of layers composed of La1/Ge1 and La2/Ge2 sites, respectively. In the former layers (labeled α) in Figure 3b, La1 and Ge1 sites are the special positions of (0, 0, 0) and (1/2, 0, 0), respectively. Since the arrangement is perfectly identical to the closest packing one, the distances of La1−Ge1 and Ge1−Ge1 are identical (3.188(1) Å). The distance between Ge1 atoms is much greater than that between diamond Ge atoms (2.447 Å). Each Ge1 atom has eight Ge neighbors: four Ge1 atoms in the same layer and four Ge2 atoms in adjacent layers. The Ge1−Ge2 distance of 2.944(3) Å is slightly shorter than that between Ge1 atoms. The La1 site has 12 neighbors: 6 Ge1 and 6 Ge2 atoms with a separation of 3.188(1) and 3.229(6) Å, respectively.

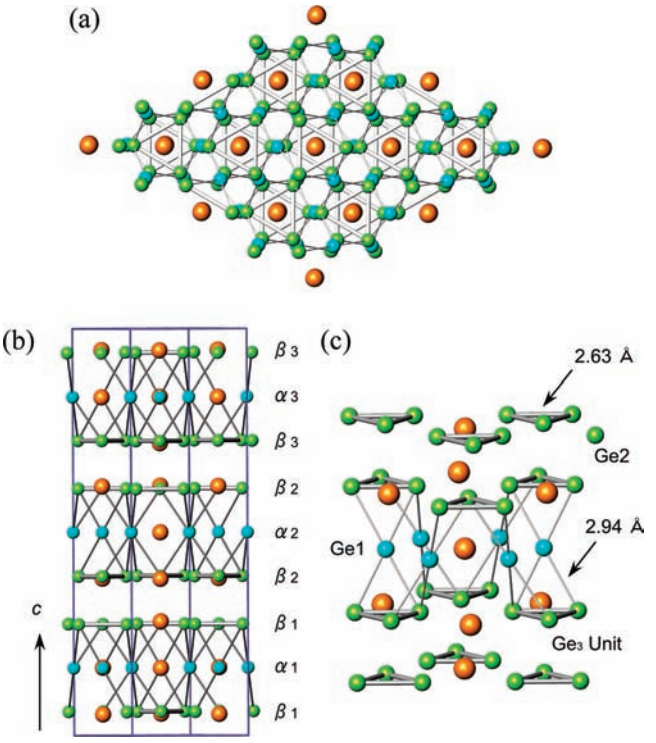

Figure 3. Crystal structure of $LaGe_3$. Projection view (a) along the c axis and (b) perpendicular to the c axis. (c) Ge_3 triangular units and their connection to the Ge1 atoms are shown in ball and stick representation. La1 and La2 atoms are situated in the same layers of Ge1 and Ge2, respectively.

In the β layers formed by La2 and Ge2 sites, the Ge atoms form a cluster having a regular triangle shape as shown in Figure 3c. Therefore, the structure of this layer is not very similar to that of the closest packing one. The Ge2−Ge2 distance of 2.634(7) Å is comparable to those in typical germanides. Each Ge2 atom has two Ge2 atoms as its nearest neighbors and two Ge1 and two Ge2 atoms as its second and third nearest neighbors with distances of 2.944(3) and 3.030(6) Å, respectively. Each La2

dx.doi.org/10.1021/ic102077k |*Inorg. Chem.* 2011, 50, 3901–3906

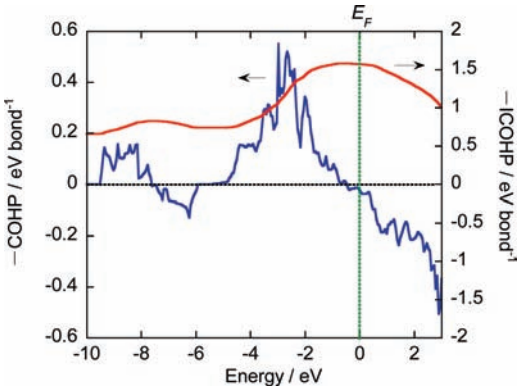

Figure 4. COHP and ICOHP diagram of $LaGe_3$ for the Ge2−Ge2 bond with a distance of 2.634 Å.

atom is surrounded by 12 Ge atoms with distances of 3.175−3.257 Å. The La2 site is situated in the relatively large space due to formation of the triangle unit of Ge2 atoms. This would be the reason why the La2 site has a large thermal displacement parameter.

To examine whether there was a covalent interaction between the Ge2 atoms in the triangular units, we performed COHP calculations using the TB-LMTO-ASA program. Figure 4 shows the COHP and ICOHP diagrams for the Ge2−Ge2 pair with a distance of 2.634(7) Å. The bonding and antibonding natures of COHP changed close to the Fermi level (E_F), indicating that the electrons on the Ge_3 unit are accommodated in bonding and nonbonding orbitals. The −ICOHP value of 1.5 eV/bond at E_F clearly shows that there is a significant interaction between the Ge2 atoms. In other words, the Ge2 atoms in the Ge_3 unit are held together by Ge2−Ge2 covalent bonds. On the other hand, the dominant interactions for Ge1−Ge1 and Ge1−Ge2 pairs in the vicinity of E_F are antibonding. The −ICOHP values for these pairs, 0.41 and 0.67 eV/bond for Ge1−Ge1 and Ge1−Ge2 with distances of 3.188(1) and 2.944(3) Å, respectively, are much smaller than that of the Ge2−Ge2 pair, suggesting there are no significant covalent interactions between the Ge1−Ge1 and Ge1−Ge2 pairs.

We performed electron localization function (ELF) analysis of $LaGe_3$ to further investigate the electrical structure of the Ge_3 triangular unit. Figure 5 shows an ELF image for the plane containing Ge_3 triangular units. The blue areas with high ELF values (η = 0.6) at each corner of the Ge_3 triangle confirm the existence of a lone pair at each Ge atom. Another area with high ELF values around η = 0.55 is also seen at the middle point of each Ge−Ge bond, corresponding to the bonding (covalent) electrons. The ELF analysis of the plane on which the Ge1 and La1 atoms are located shows no significant structures, indicating that the Ge1 atoms are almost in an isolated condition, and there is no covalent interaction between Ge1 atoms. Furthermore, no evidence for bonding between Ge1 and Ge2 was obtained by ELF calculations. These results were in good agreement with the COHP analysis described above.

Subunits like the Ge_3 triangle are often observed in AB_3-type intermetallic compounds. The $SrSn_3$ and $BaSn_3$ structures contain Sn_3 triangular units.[38,40] The structures of $SrSn_3$ and $BaSn_3$ are similar to that of $LaGe_3$. They are built from the closest-packed like layers, but the stacking sequences of the three compounds are different. $SrSn_3$ crystallizes in a trigonal unit cell

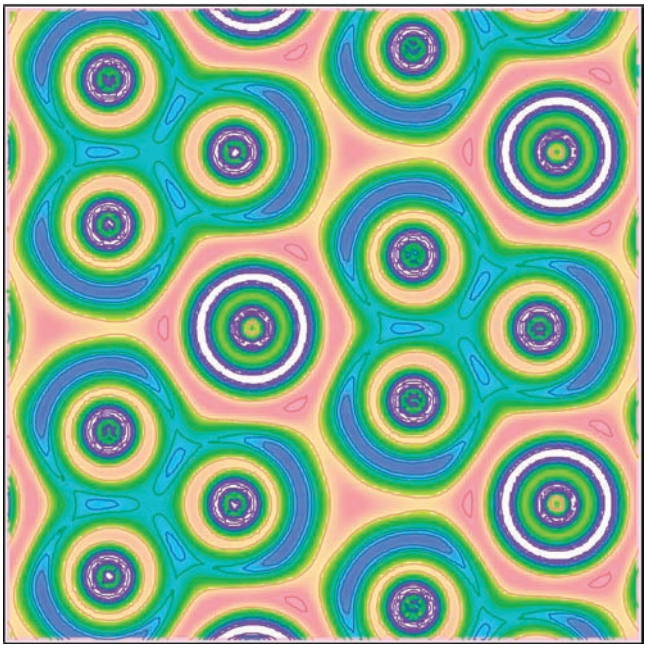

Figure 5. Electron localization function (ELF) diagram of $LaGe_3$ for the plane parallel to the *ab* plane at z = 0.1076 on which Ge2 and La2 atoms are situated. Red and blue colors show the low and high ELF areas, respectively.

with space group $R\bar{3}m$. $BaSn_3$ crystallizes in a hexagonal unit cell with $P6_3/mmc$. $LaGe_3$, $SrSn_3$, and $BaSn_3$ contain 9, 12, and 2 closest packed layers in their respective unit cells. ELF analysis of $SrSn_3$ and $BaSn_3$ by Fässler et al. revealed that the Sn_3 triangular units have attractors corresponding to lone pairs and covalent bonding electrons.[38,40] The ELF image of the Ge3 unit in $LaGe_3$ is similar to those of the other structures.

The temperature dependence of the resistivity is shown in Figure 6. The resistivity of $LaGe_3$ decreases with decreasing temperature down to about 8 K and then slightly increases followed by zero resistivity below 7.4 K. This trend indicates that $LaGe_3$ is metallic and shows superconductivity with transition temperature T_c = 7.4 K. The magnetic susceptibility measurements also confirmed the superconducting transition as shown in Figure 7. The temperature dependence curve of the magnetic susceptibility of $LaGe_3$ passes through zero magnetization at 7.4 K and then shows a rapid decrease to negative values in agreement with the results of the conductivity measurements. The superconducting volume fraction calculated from the plot in Figure 7 is more than 100% at 2 K, clearly showing that the transition is due to $LaGe_3$. $BaSn_3$ and $SrSn_3$ also show superconductivity at T_c = 4.3 and 5.4 K, respectively. The structures based on the closest packing layers of electropositive metals and group 14 elements might be advantageous for the appearance of superconductivity.

From specific heat measurement of $LaGe_3$, the superconducting specific heat jump ΔC_v = 82 mJ K^{-1} mol^{-1} was observed at 7.0 K. If we assume this compound to be a BCS-type superconductor, the electronic specific heat coefficient, γ, of 7.7 mJ K^{-2} mol^{-1} is obtained.

To obtain a theoretical view for the electrical properties of $LaGe_3$, we performed the density of state (DOS) and band calculations using the Wien2k package. The DOS diagram of $LaGe_3$ in Figure 8 clearly shows the metallic properties of this compound. The low-lying bands below −5 eV are mostly

dx.doi.org/10.1021/ic102077k |*Inorg. Chem.* 2011, 50, 3901–3906

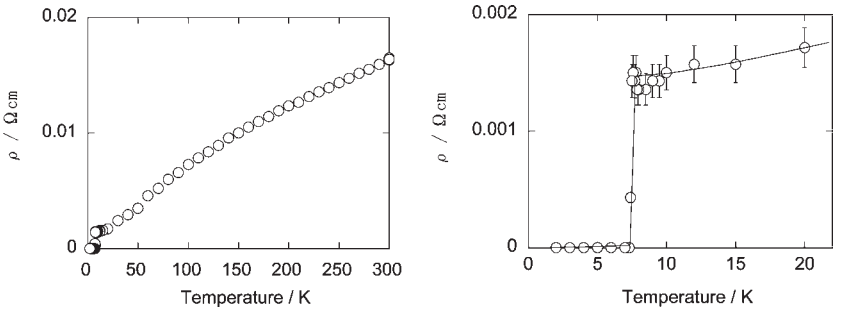

Figure 6. Temperature dependence of the electrical resistivity for $LaGe_3$ for a (a) wide temperature range and (b) lower temperature range.

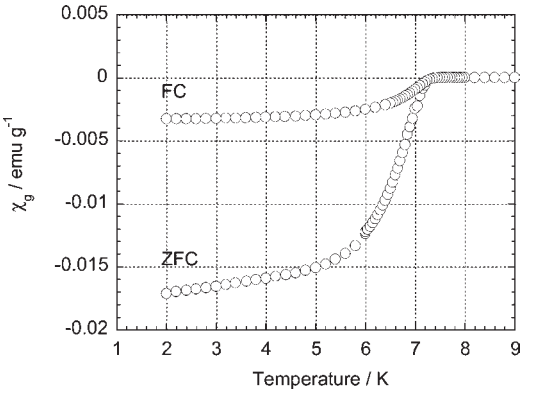

Figure 7. Temperature dependence of the magnetic susceptibility of $LaGe_3$.

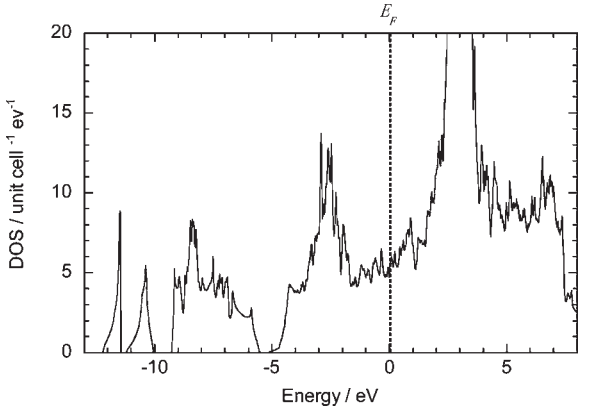

Figure 8. Density of states (DOS) for $LaGe_3$ obtained from LAPW calculations (the Wien2k code). The Fermi level is set as zero.

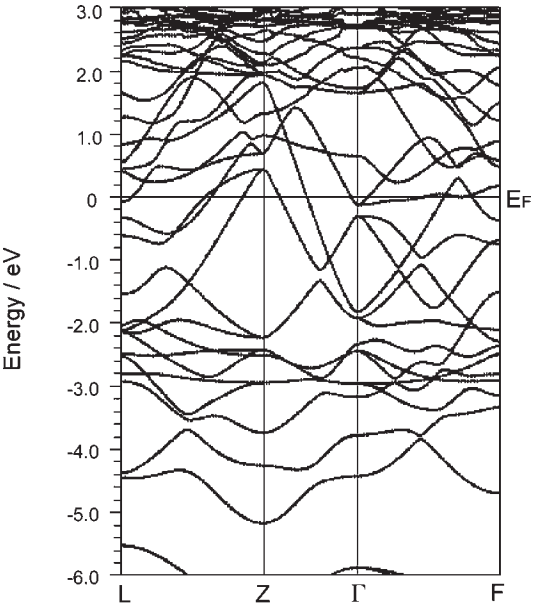

Figure 9. Band structure diagram of $LaGe_3$.

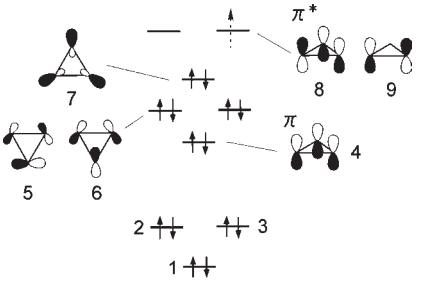

Figure 10. Schematic molecular orbitals of Sn_3^{2-} triangular unit proposed by Fässler et al. If the ionic valence of the Ge_3 triangle in $LaGe_3$ is −3, an electron displayed by a dotted arrow will be added to the π^* orbital.

contributed by Ge 4s orbitals, and the bands above −5 eV up to E_F contain the contributions of Ge 4p, La 5d, and the interstitial components. A portion of the doped electrons from the La^{3+} ions are accommodated in the empty Ge 4p orbitals to be as localized electrons, and the remainder becomes itinerant electrons, the orbitals of which contain both Ge and La contributions. A small contribution from the La 4f orbitals at around E_F was admitted in the calculations, but it is uncertain whether this contribution is essential or just artificial.

The band structure (k dispersion) of $LaGe_3$ is presented in Figure 9. Several bands cross E_F not only along the Z → Γ pass (corresponding to the direction of the z axis) but also along the L → Γ and Γ → F passes, indicating that $LaGe_3$ is not a 1D conductor. The Fermi surfaces sprawl in many directions of the Brillion zone, and their shapes are complicated.

Finally, we discuss the scheme of the electronic structure of $LaGe_3$. Fässler et al. proposed an electronic structure model for the Sn_3^{2-} unit in $SrSn_3$ and $BaSn_3$ based on the molecular orbital (MO) scheme. They deduced the model from the MO of aromatic 2π-electron cyclopropanyl cations ($C_3R_3^+$) because this cation is isoelectronic with Sn_3^{2-}. Figure 10 depicts this MO scheme. According to this model, the Sn_3^{2-} anion has three lone pairs (orbitals 5, 6, and 7) and one π-bonding pair (orbital 4).

dx.doi.org/10.1021/ic102077k |Inorg. Chem. 2011, 50, 3901–3906

In the case of $LaGe_3$, the Ge2 atoms form Ge_3 triangular units. In the ELF and COHP analyses, the triangular unit has three lone pairs as well as three covalent bonds. If the units were completely isolated from the environment, the π and π^* orbitals (4, 8, and 9) would be localized on the unit. In fact, the π and π^* orbitals of the $Ge2_3$ unit are reconstructed into the conduction bands by combination with the orbitals of other $Ge2_3$ units and Ge1 atoms in the adjacent layers, and the electrons presupposed to be accommodated in the π^* orbitals are delocalized to become conduction electrons. These conduction bands contain the contribution of the orbitals of the La1 and La2 atoms, resulting in 3D bands.

CONCLUSIONS

Reactions of $LaGe_2$ and Ge under high-pressure and high-temperature conditions yielded a new superconducting lanthanum germanide, $LaGe_3$, with $T_c = 7.4$ K. This temperature is the highest T_c value among the compounds of the La−Ge binary system at present. The structure is based on stacking of the closest packed layers of La and Ge atoms. There are two types of layers: one is composed of La1 and Ge1 equidistant from each other, and the other is composed of La2 and $Ge2_3$ triangular cluster units. ELF and COHP analyses revealed that the triangle unit is constructed by Ge2−Ge2 covalent bonds and that each Ge2 atom has a lone pair of electrons. This is the first triangular Zintl anion of Ge to our knowledge. The results of the band structure calculation supported the fact that this compound possesses metallic properties.

AUTHOR INFORMATION

Corresponding Author

*Phone: +81-824-24-7742. Fax: +81-824-24-5494. E-mail: hfukuoka@hiroshima-u.ac.jp.

ACKNOWLEDGMENT

We are grateful to Mr. Yasuhiro Shibata of Hiroshima University for his help with the EPMA measurements. This work was supported by a Grant-in-Aid for Scientific Research from the Ministry of Education, Science, and Culture of Japan, Grant Nos. 16037212, 16750174, 18750182, 18027010, and 20550178.

REFERENCES

(1) Kauzlarich, S. M.; Kniep, R.; Miller, G. J.; Eisenmann, B.; Cordier, G.; Corbett, J. D. et al. *Chemistry, Structure, and Bonding of Zintl Phases and Ions*; VCH Publishers Inc.: New York, 1996.
(2) Corbett, J. D. *Angew. Chem., Int. Ed.* **2000**, *39*, 670–690.
(3) Vaughey, J. T.; Miller, G. J.; Gravelle, S.; Leon−Escamilla, E. A.; Corbett, J. D. *J. Solid State Chem.* **1997**, *133*, 501–507.
(4) Tegze, M.; Hafner, J. *Phys. Rev.* **1989**, *B40*, 9841–9845.
(5) Klem, M. T.; Vaughey, J. T.; Harp, J. G.; Corbett, J. D. *Inorg. Chem.* **2001**, *40*, 7020–7026.
(6) Bobev, S.; Bauer, E. D.; Thompson, J. D.; Sarrao, J. L.; Miller, G. J.; Eck, B.; Dronskowski, R. *J. Solid State Chem.* **2004**, *177*, 3545–3552.
(7) Yamanaka, S.; Enishi, E.; Fukuoka, H.; Yasukawa, M. *Inorg. Chem.* **2000**, *39*, 56.
(8) Cros, C.; Pouchard, M.; Hagenmuller, P. *J. Solid State Chem.* **1970**, *2*, 570–581.
(9) Kasper, J. S.; Hargenmuller, P.; Pouchard, M.; Cros, C. *Science* **1965**, *150*, 1713–1714.
(10) Cros, C.; Pouchard, M. *C. R. Chimie* **2009**, *12*, 1014–1056.
(11) von Schnering, H.-G. *Nova Acta Leopold.* **1985**, *59*, 168.
(12) Zintl, E. *Angew. Chem.* **1939**, *52*, 1.
(13) Klemm, W.; Busmann, E. *Z. Anorg. Allgem. Chem.* **1963**, *319*, 297.
(14) Eisenmann, B.; Schäfer, H.; Zagler, R. *J. Less-Common Met.* **1986**, *118*, 43–55.
(15) Cordier, G.; Woll, P. *J. Less−Common Met.* **1991**, *169*, 291–303.
(16) Cabrera, W. C.; Curda, J.; Peters, K.; Pashen, S.; Baenitz, M.; Grin, Y.; von Schnering, H.-G. *Z. Kristallogr. New Cryst.* **2000**, *215*, 321.
(17) Fukuoka, H.; Kiyoto, J.; Yamanaka, S. *J. Solid State Chem.* **2003**, *175*, 237–244.
(18) Okamoto, N. L.; Tanaka, K.; Inui, H. *Acta Mater.* **2006**, *54*, 173–178.
(19) Aydemir, U.; Candolfi, C.; Borrmann, H.; Baitinger, M.; Ormeci, A.; Carrillo−Cabrera, W.; Chubilleau, C.; Lenoir, B.; Dauscher, A.; Oeschler, N.; Steglich, F.; Grin, Y. *Dalton Trans.* **2010**, *39*, 1078–1088.
(20) Herrmann, R. F. W.; Tanigaki, K.; Kikuchi, T.; Kuroshima, S.; Zhou, O. *Phys. Rev.* **1999**, *B60*, 13245.
(21) Fukuoka, H.; Kiyoto, J.; Yamanaka, S. *Inorg. Chem.* **2003**, *42*, 2933–2937.
(22) Kitano, A.; Moriguchi, K.; Yonemura, M.; Munetoh, S.; Shintani, A.; Fukuoka, H.; Yamanaka, S.; Nishibori, E.; Takata, M.; Sakata, M. *Phys. Rev.* **2001**, *B64*, 0452061–0452069.
(23) Itou, M.; Sakurai, Y.; Usuda, M.; Cros, C.; Fukuoka, H.; Yamanaka, S. *Phys. Rev.* **2005**, *B71*, 1251251–1251254.
(24) Shimizu, H.; Kume, T.; Kuroda, T.; Sasaki, S.; Fukuoka, H.; Yamanaka, S. *Phys. Rev.* **2005**, *B71*, 0941081–0941085.
(25) San−Miguel, A.; Toulemonde, P. *High Press. Res.* **2005**, *25*, 159–185.
(26) Fukuoka, H.; Ueno, K.; Yamanaka, S. *J. Organomet. Chem.* **2000**, *611*, 543–546.
(27) Rachi, T.; Yoshino, H.; Kumashiro, R.; Kitajima, M.; Kobayashi, K.; Yokogawa, K.; Murata, K.; Kimura, N.; Aoki, H.; Fukuoka, H.; Yamanaka, S.; Shimotani, H.; Takenobu, T.; Iwasa, Y.; Sasaki, T.; Kobayashi, N.; Miyazaki, Y.; Saito, K.; Guo, F.; Kobayashi, K.; Osaka, K.; Kato, K.; Takata, M.; Tanigaki, K. *Phys. Rev.* **2005**, *B72*, 144504.
(28) Fukuoka, H.; Yamanaka, S. *Phys. Rev.* **2003**, *B67*, 0945011–0945015.
(29) Fukuoka, H.; Iwai, K.; Yamanaka, S.; Abe, H.; Yoza, K.; Haming, L. *J. Solid State Chem.* **2000**, *115*, 117.
(30) Carrillo−Cabrera, W.; Curda, J.; Paschen, S.; Von Schnering, H. G. *Z. Kristallogr.* **2000**, *215*, 207.
(31) Kim, S.−J.; Hu, S.; Uher, C.; Hogan, T.; Huang, B.; Corbett, J. D.; Kanatzidis, M. G. *J. Solid State Chem.* **2000**, *153*, 321.
(32) Aydemir, U.; Akselrud, L.; Carrillo-Cabrera, W.; Candolfi, C.; Oeschler, N.; Baitinger, M.; Steglich, F.; Grin, Y. *J. Am. Chem. Soc.* **2010**, *132*, 10984.
(33) Fukuoka, H.; Baba, K.; Yoshikawa, M.; Ohtsu, F.; Yamanaka, S. *J. Solid State Chem.* **2009**, *182*, 2024–2029.
(34) Fukuoka, H. *Rev. High Press. Sci. Technol.* **2006**, *16*, 329.
(35) Izumi, F.; Ikeda, T. *Mater. Sci. Forum* **2000**, *321−324*, 198–203.
(36) Blaha, P.; Schwarz, K.; Madesen, G. K. H.; Kvasnicka, D.; Luitz, J. *Wien2k, An Augmented Plane Wave + Local Orbitals Program for Calculating Crystal Properties*; Karlheinz Schwarz, Techn. Universität Wien: Austria, 2001.
(37) Jepsen, O.; Burkhardt, A.; Andersen, O. K. *The Program TB-LMTO*, version 4.7; Max−Planck Institute für Festkörperforschung: Stuttgart, 1999.
(38) Fässler, T. F.; Kronseder, C. *Angew. Chem., Int. Ed. Engl.* **1997**, *36*, 2683–2686.
(39) Sands, D. E.; Wood, D. H.; Ramsey, W. J. *Acta Crystallogr.* **1964**, *17*, 986–989.
(40) Fässler, T. F.; Hoffmann, S. *Z. Anorg. Allg. Chem.* **2000**, *626*, 106–112.